Reprinted from J. Aud. Eng. Soc.
23 No. 3, April 1975 with
permission of the author

The Frequency Modulation Spectrum of an Exponential Voltage-Controlled Oscillator*

BERNARD A. HUTCHINS, JR.

Electronotes, Ithaca, N. Y. 14850

As the amplitude of a modulating voltage to an exponential VCO is increased, the pitch of the modulated signal rises, making dynamic depth FM unrealistic. The pitch rise is proportional to I_0, the first of the modified Bessel functions. Higher order terms involving additional modified Bessel functions can be used to compute the entire spectrum. Various methods of correcting for the pitch shift are possible, but the most useful solution to the dynamic depth FM problem with exponential VCO's is to add some form of auxiliary linear control.

INTRODUCTION: Exponential voltage-controlled oscillators (E-VCOs) are those which produce a frequency which is an exponential function of the control voltage. Ever since the advantages of E-VCOs in musical systems were pointed out [1], it has been realized, and at times noted [2] that the straightforward frequency modulation (FM) patch would not produce a spectrum that could be calculated from the well understood FM radio broadcasting theory. The radio equations apply to a linear voltage-controlled oscillator (L-VCO), not an E-VCO.

SIMPLE MODULATION PATCHES

However, imperfect understanding of the exact details of the E-VCO FM spectrum does not prevent use of the method. For example, the patch shown in Fig. 1 has proven useful for the production of clangorous sounds which have a tone quality that does not vary with pitch. Recently, Chowning [3] used a digital computer method to demonstrate an FM synthesis method where the depth of modulation changes dynamically as a tone progresses. The method employs the equivalent of an L-VCO. In the apparently straightforward realization of this dynamic depth FM method using standard analog music synthesizers (hence E-VCOs), one tries a patch such as the one in Fig. 2. The amplitude of the modulating signal is controlled by a voltage-controlled amplifier (VCA) that is in turn controlled by an approp-

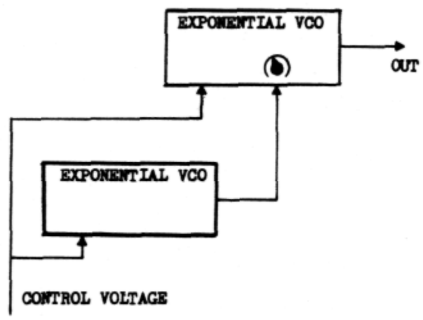

Fig. 1. Patch for clangorous sounds.

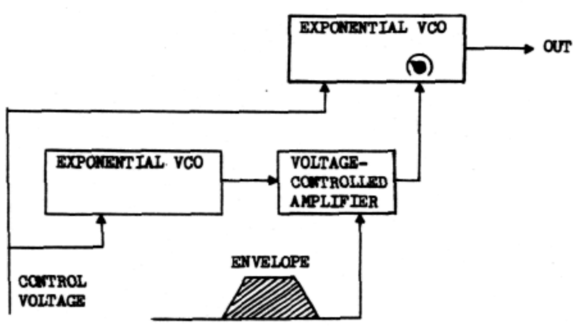

Fig. 2. Dynamic depth FM patch that produces pitch change.

* An earlier version of the paper was presented September 12, 1974, at the 49th Convention of the Audio Engineering Society, New York.

riate envelope. A problem immediately arises in that the E-VCO spectrum undergoes an overall pitch shift as modulation depth changes. While this can be a useful special effect, in general it is disconcerting.

CALCULATING THE E-VCO SPECTRUM

Attempts to use a dynamic depth FM method have made consideration of the E-VCO FM problem more important. A thorough analysis of the problem is useful for electronic music engineers as it both defines the problem and suggests solutions, and will also provide the engineer with a means of fielding questions from musicians who note the unusual behavior of their synthesizers.

The E-VCO FM problem is, like all FM problems, actually a phase modulation problem. This can be visualized as a rotating vector of constant magnitude, where the orientation angle of the vector is $A(t)$ as shown in Fig. 3. The signal voltage is then proportional to $\sin A(t)$. The time rate of change of $A(t)$ is then proportional to what is termed the instantaneous frequency:

$$2\pi F_{\text{inst}} = dA(t)/dt. \tag{1}$$

In the L-VCO case, the instantaneous frequency is proportional to the control voltage $V(t)$:

$$F_{\text{inst}} = f_0 V(t). \tag{2}$$

For the standard E-VCO (1 volt per octave), the control voltage appears in the exponent, which has a base of two:

$$F_{\text{inst}} = f_0 2^{V(t)} = f_0\, e^{\ln 2 \cdot V(t)}. \tag{3}$$

It is convenient to start with a control voltage that varies as a cosine:

$$V(t) = V_0 + V_m \cos(2\pi f_m t) \tag{4}$$

where V_m is the amplitude of the modulating voltage and f_m is the modulating frequency. In the L-VCO case, this gives a constant-center frequency (the carrier) and a modulation depth ΔF.

$$\frac{1}{2\pi}\frac{dA(t)}{dt} = F_{\text{inst}} = f_0 V_0 + f_0 V_m \cos 2\pi f_m t$$
$$= F_{\text{CL}} + \Delta F \cos 2\pi f_m t. \tag{5}$$

This can be easily integrated to give the well-known FM radio equation:

$$E(t) = \sin A(t) = \sin\left[2\pi F_{\text{CL}} + \frac{\Delta F}{f_m}\sin 2\pi f_m t\right]t. \tag{6}$$

In the E-VCO case, cosine modulation gives:

$$F_{\text{inst}} = f_0 \exp\{\ln 2\cdot(V_0 + V_m \cos 2\pi f_m t)\}$$
$$= F_{\text{CE}} \exp\{\ln 2\cdot V_m \cos 2\pi f_m t\}. \tag{7}$$

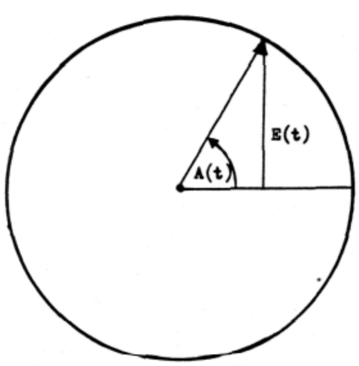

Fig. 3. Rotating vector model of phase modulation.

The exponential factor can be expanded according to the series [4]

$$e^{z\cos\theta} = I_0(z) + 2\sum_{k=1}^{\infty} I_k(z)\cos k\theta \tag{8}$$

where the Fourier coefficients are fortunately tabulated functions known as modified Bessel functions, or hyperbolic Bessel functions. The E-VCO expression for F_{inst} can then be integrated as in the L-VCO case to give $A(t)$, and $E(t)$ then becomes

$$E(t) = \sin\,[\,2\pi\; F_{\text{CE}}\, I_0\,(\ln 2\cdot V_m)t$$
$$+ \sum_{k=1}^{\infty} (2\cdot F_{\text{CE}} / k\cdot f_m)\, I_k\,(\ln 2\cdot V_m)\sin 2\pi k f_m t]. \tag{9}$$

The first five modified Bessel functions are shown in Fig. 4. The modified Bessel functions are related to the better known Bessel functions of the first kind J_n by the relation

$$I_n(z) = i^{-n} J_n(iz). \tag{10}$$

I_0 is very important as it will eventually be seen to determine the overall position of the FM spectrum. The higher order I_n terms are an indication of the number of terms that must be retained for a given degree of accuracy in the spectral calculations.

A form of the FM equation that is more useful than Eq. (6), or Eq. (9) in the E-VCO case, is the one that reveals the spectrum of the signal, as this is the one most easily related to the hearing process. Conversion of the modulation equation to a spectral equation is well known in the L-VCO case [5]. A modulation index m is defined as $\Delta F/f_m$, and a series of five identities, Eqs. (11)–(15), are applied to Eq. (6):

$$\sin(x+y) = \sin(x)\cdot\cos(y) + \cos(x)\cdot\sin(y) \tag{11}$$

$$\sin[m\,\sin(x)] = 2[J_1(m)\sin(x) + J_3(m)\sin(3x) + J_5(m)\sin(5x) + \cdots] \tag{12}$$

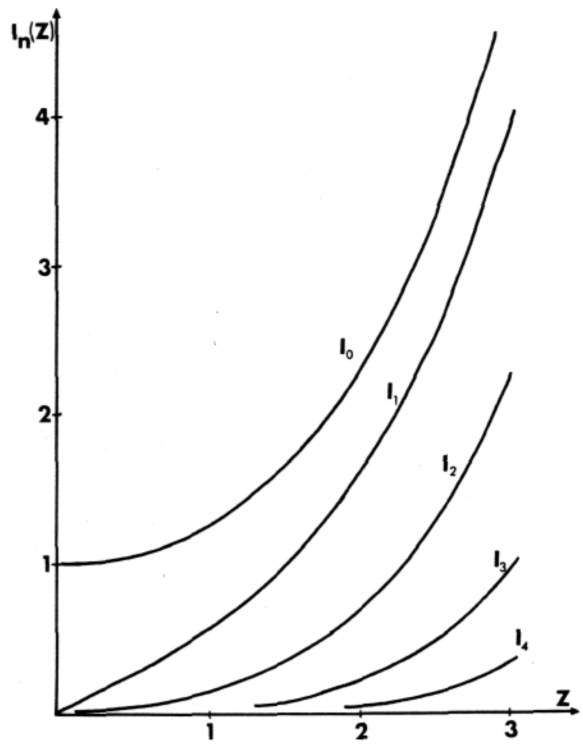

Fig. 4. First five modified Bessel functions.

$$\cos[m \sin(x)] = J_0(m) + 2\,[J_2(m)\cos(2x) + J_4(m)\cos(4x) + \cdots] \tag{13}$$

$$\sin(x)\cdot\cos(y) = \tfrac{1}{2}[\sin(x+y) + \sin(x-y)] \tag{14}$$

$$\cos(x)\cdot\sin(y) = \tfrac{1}{2}[\sin(x+y) - \sin(x-y)] \tag{15}$$

The spectral equation then becomes

$$\begin{aligned} E(t) = {} & J_0(m) \sin 2\pi F_{CL}\, t \\ & + J_1(m)\,[\sin 2\pi\,(F_{CL} + f_m)t \\ & - \sin 2\pi\,(F_{CL} - f_m)t] \\ & + J_2(m)\,[\sin 2\pi\,(F_{CL} + 2f_m)t \\ & + \sin 2\pi\,(F_{CL} - 2f_m)t] \\ & + \cdots . \end{aligned} \tag{16}$$

The J_n are Bessel functions of the first kind. The spectral equation thus shows that a series of sidebands are formed about the carrier, and since $J_{-n} = (-1)^n J_n$, the spectrum is symmetric about the carrier with respect to the absolute values of the amplitudes. Conservation of spectrum energy is demonstrated by the Bessel function identity

$$1 = J_0^2 + 2 \sum_{k=1}^{\infty} J_k^2. \tag{17}$$

A typical spectrum is shown in Fig. 5 for the L-VCO case.

In the E-VCO case the calculations are greatly complicated by the additional terms. Consider first a limited case where I_2 is still negligible. The E-VCO modulation equation, Eq. (9), then becomes

$$\begin{aligned} E(t) = {} & \sin\,[2\pi F_{CE} I_0 (\ln 2\cdot V_m)t \\ & + (2 F_{CE}/f_m)\, I_1(\ln 2\cdot V_m) \sin 2\pi f_m t]. \end{aligned} \tag{18}$$

This has the same mathematical form as the L-VCO equation with

$$F_{CL} \rightarrow F_{CE} I_0 (\ln 2\cdot V_m) \tag{19}$$

$$m \rightarrow (2 F_{CE}/f_m)\, I_1(\ln 2\cdot V_m) \cong 0.69\, V_m (F_{CE}/f_m). \tag{20}$$

In this linear approximation, which is quite good for V_m less than half a volt, sideband positions and amplitudes about the carrier are calculated according to the L-VCO equations, and then placed about a carrier that has slid up the I_0 curve according to the magnitude of V_m.

It turns out that even when more terms are considered in the E-VCO equation, the entire spectrum still shifts along the I_0 curve as shown in Fig. 6. This replot of the I_0 function has additional labels to show the $\ln 2\cdot V_m$ axis, as well as the total frequency deviation and spectrum slide in units of semitones. It is the shift implied by this curve that is responsible for the (generally) annoying pitch variation that occurs as modulation depth changes while a tone progresses.

When three or more terms must be kept, calculations must go beyond the simple expansion about the L-VCO solution. For example, when I_4 can be neglected, but not I_3, the modulation equation becomes

$$\begin{aligned} E(t) = {} & \sin\,[\,2\pi F_{CE} I_0 (\ln 2\cdot V_m)t + m_1 \sin 2\pi f_m t \\ & + m_2 \sin 4\pi f_m t + m_3 \sin 6\pi f_m t] \end{aligned} \tag{21}$$

where

$$m_1 = (2 F_{CE}/f_m)\, I_1(\ln 2\cdot V_m) \tag{22a}$$

$$m_2 = (F_{CE}/f_m)\, I_2(\ln 2\cdot V_m) \tag{22b}$$

$$m_3 = (2 F_{CE}/3f_m)\, I_3(\ln 2\cdot V_m). \tag{22c}$$

It is interesting that this equation has the same form that is obtained by considering the simultaneous modulation of a L-VCO with more than one sine wave. This can be understood by considering that the E-VCO expression for F_{inst} could be duplicated by applying an appropriate periodic waveform to the L-VCO. In the E-VCO case, the additional sine waves are all harmonically related, but the more general problem was considered as far back as 1938 [6]. The solution consists of the application of Eq. (11) and its corresponding identity

$$\cos(x+y) = \cos(x)\cdot\cos(y) + \sin(x)\cdot\sin(y) \tag{23}$$

to Eq. (21), considering the first term as x and the remaining terms as y, and repeating this process until all the terms are used up. The final result is [7]

$$E(t) = \sum_{k_s=-\infty}^{\infty} \left[\prod_{s=1}^{S} J_{k_s}(m_s) \right] \times \sin\,[2\pi I_0 (\ln 2\cdot V_m) F_{CE} + \sum_{s=1}^{S} 2\pi k_s f_m\,]\,t. \tag{24}$$

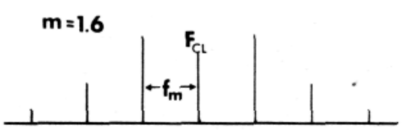

Fig. 5. A typical L-VCO spectrum.

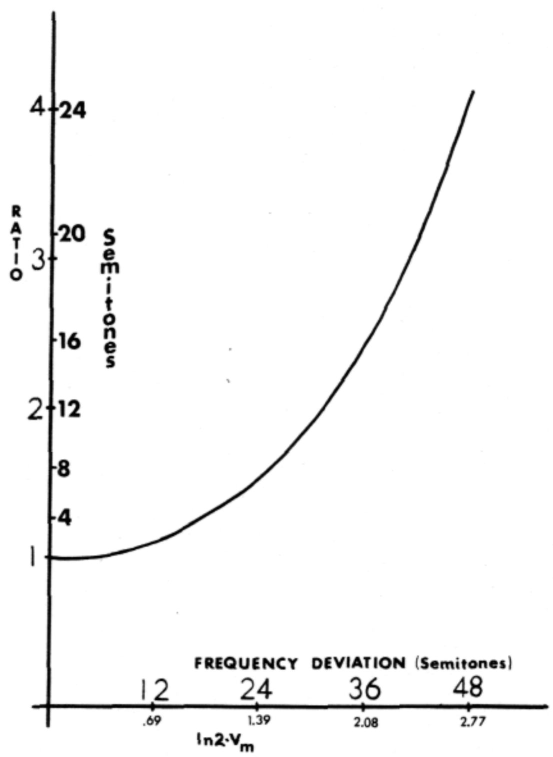

Fig. 6. Shift of spectrum with increasing modulation voltage V_m.

2c (15)

For the four-term case, this equation can be greatly reduced:

$$E(t) = \sum_{L=-U}^{U} \sum_{M=-U}^{U} \sum_{N=-U}^{U} \Big[J_L(m_1)\, J_M(m_2)\, J_N(m_3)$$

$$\times \sin 2\pi \,[I_0 (\ln 2 \cdot V_m)\, F_{CE}$$

$$+ Lf_m + 2Mf_m + 3Nf_m \,]\, t \Big]. \tag{25}$$

In the above equation, U is the highest order L index which must be considered, corresponding to the smallest J_L which is still significant. To further simplify the calculations, consideration of the overall spectrum shift can be set aside and added in later. For computer calculations, the procedure is then as follows.

1) Select V_m and the ratio F_{CE}/f_m.

2) Determine all significant values of $I_n(\ln 2 \cdot V_m)$.

3) From the I_n values, calculate m_1, m_2, m_3, $\cdots$ and from these, calculate all significant values of $J_n(m_k)$.

4) Execute a nested "do loop" for each summation, three in the case of Eq. (25), and inside the innermost do loop

a) Determine the sideband in question: $L + 2M + 3N$;

b) Calculate $J_L(m_1)\, J_M(m_2)\, J_N(m_3)$ and add this to any previous contribution for the same sideband.

5) Reposition the sidebands. Space them at intervals of f_m about the carrier (zeroth sideband) shifted according to $I_0(\ln 2 \cdot V_m)$.

6) Any sideband that has a negative frequency should be changed to a positive frequency and be considered reflected back into the positive spectrum according to $\sin(-x) = -\sin(x)$.

EXPERIMENTAL VERIFICATION

These theoretical calculations can be verified with an experimental setup employing a spectrum analizer. A redrawn version of an experimental spectrogram is shown in Fig. 7. The predicted spacing of the sidebands at intervals of f_m and the predicted spectrum slide is observed. Also, the linearlike structure for $V_m = 0.5$ and the much more complicated pattern for $V_m = 1$ can be seen. In particular, there are more significant sidebands above the carrier than below.

Fig. 8 shows a plot of calculated and experimental sideband amplitudes for some 47 sidebands from six different E-VCO spectra. The agreement is within expected experimental and computational accuracy.

EXAMPLE SPECTRA

With this experimental verification completed, calculations can be viewed with more confidence. Fig. 9 shows a complete series of calculated amplitudes for the ratio $F_{CE}/f_m = 8$. When the ratio is lowered to 2.0, it is easier for significant sidebands to reach zero frequency and below. These sidebands are reflected back into the positive spectrum (and are experimentally observed as predicted). Such sidebands are very common in the L-VCO case, but are relatively rare in the E-VCO case for two reasons. First, the instantaneous frequency can never reach zero, and in general there are very few significant sidebands produced outside the range of F_{inst}. Second, as modulation depth increases and more and more sidebands start to appear at the extremes of the spectrum, the spectrum shifts up, pulling the lower ones away from zero. These lower sidebands often begin to become significant while in their reflected positions. In this case, as the spectrum shifts up, these sidebands are pulled down and around zero where they reemerge as normal lower sidebands. Sidebands behaving in this manner

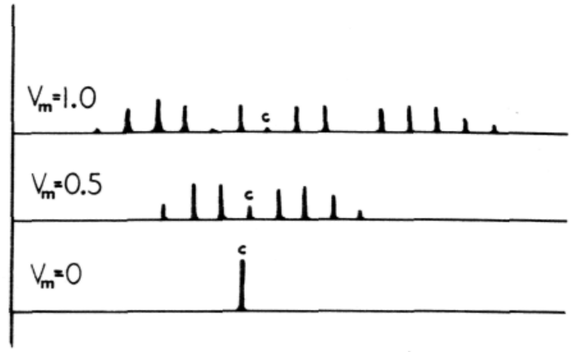

Fig. 7. Experimental spectrogram for $F_{CE}/f_m = 8$; $V_m = 0, 0.5$, and 1.0

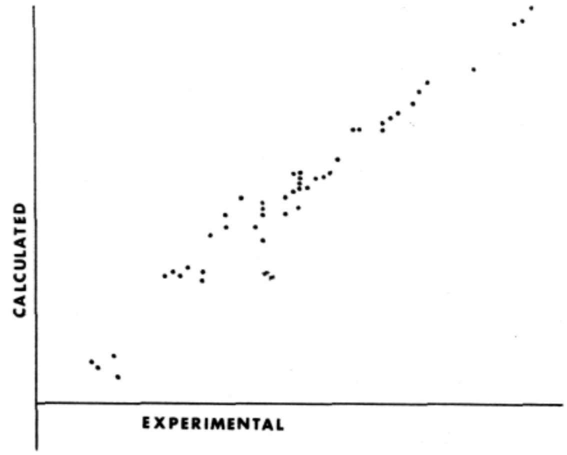

Fig. 8. Comparison of calculated and experimental sideband amplitudes.

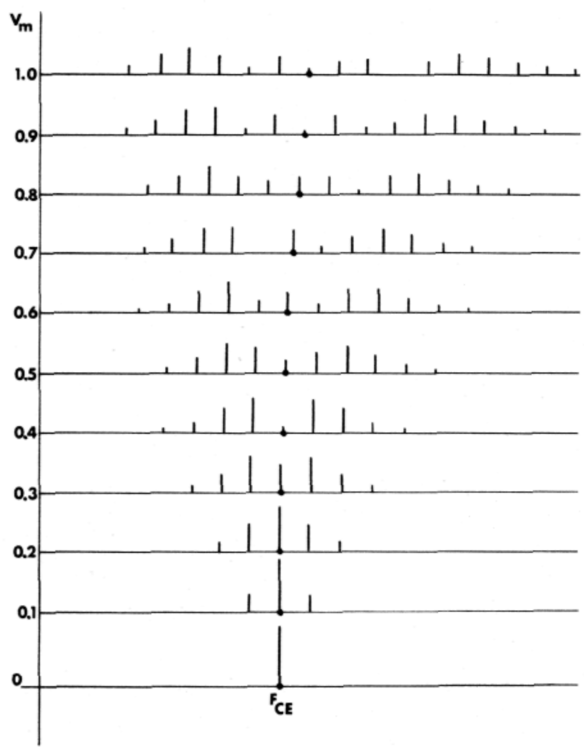

Fig. 9. Spectra for $F_{CE}/f_m = 8$.

can be seen in Fig. 10 for $F_{CE}/f_m = 2$, and in Fig. 11 for $F_{CE}/f_m = ½$.

In the process of calculation, the power in each sideband, which goes as the amplitude squared, is easy to compute and tabulate. A surprising result is noted: while there are more significant sidebands above the carrier, there is more power produced below. Both these results can perhaps be understood in terms of the graph of the E-VCO instantaneous frequency of Fig. 12. The instantaneous frequency goes much higher above the carrier than below, and therefore passes over more possible sideband positions on the high side, hence activating more of them. Although the carrier slides up with increased modulation depth (from the solid to the dotted line), the points at which the instantaneous frequency crosses at equal time intervals remain on the original carrier line. Therefore, the instantaneous frequency spends more time below the shifted carrier than above, and more power is distributed to the lower sidebands, even though there are fewer of them.

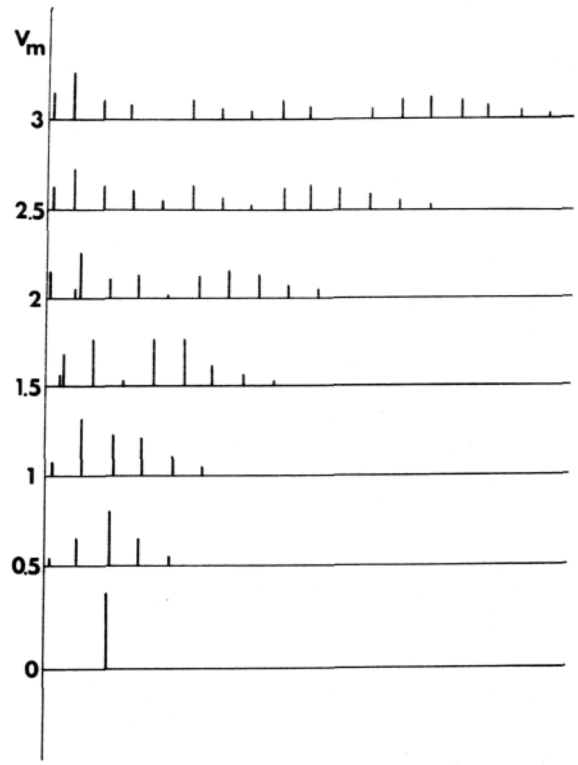

Fig. 10. Spectra for $F_{CE}/f_m = 2$.

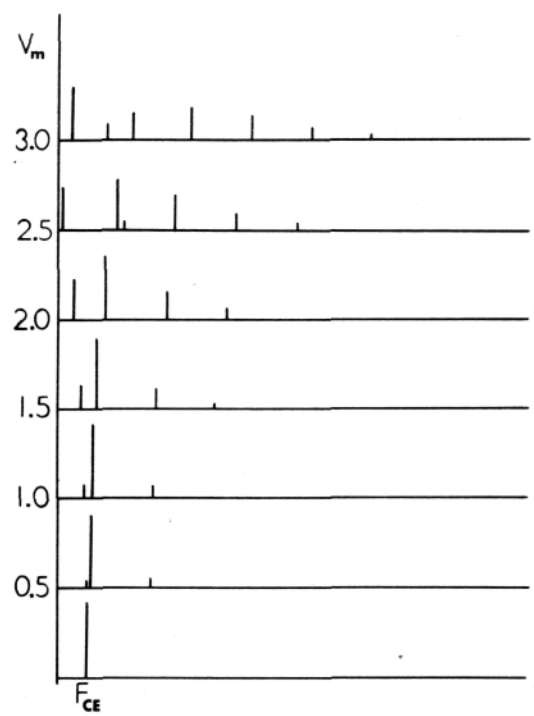

Fig. 11. Spectra for $F_{CE}/f_m = ½$.

Fig. 12 is also helpful in understanding the carrier shift along the I_0 curve. The areas between the F_{inst} curve and the shifted carrier are equal on both sides. This is equivalent to the dc level that would be required to produce the same F_{inst} curve with a L-VCO.

HARMONIC SPECTRA

An interesting application of the FM method is the production of harmonic spectra by allowing one of the sidebands to fall on zero frequency. In this case the carrier, all normal sidebands, and any significant reflected sidebands will fall on positions that are multiples of a common fundamental. In the E-VCO case, the condition for a harmonic spectrum is

$$F_{CE}/f_m = \frac{1}{I_0(\ln 2 \cdot V_m)} \cdot \frac{n_1}{n_2}$$

where n_1 and n_2 are integers. A typical harmonic spectrum is shown in Fig. 13. In the E-VCO case, unlike the L-VCO case, the condition for a harmonic spectrum is a function of V_m, making the condition impossible to maintain during dynamic depth modulation. A zero-frequency component in the harmonic spectrum actually just occurs as a dc weighting of the waveform. The actual amplitudes obtained for a harmonic spectrum depend on the relative phase of the original carrier and the modulating waveform, since reflected sidebands will have a phase that depends on these initial conditions. Control of this phase is difficult with ordinary synthesizers.

SUGGESTED SOLUTIONS

The theory presented has allowed the calculation of the E-VCO FM spectrum, and outlined the cause of the pitch shift problem encountered during dynamic depth FM. Several solutions to this problem are suggested.

A patch such as the one in Fig. 14 can be tried. Here the envelope controlling the modulation depth is inverted and used to pull the pitch back down as the modulation depth increases. When this inverted voltage is fed directly to the VCO, correction is

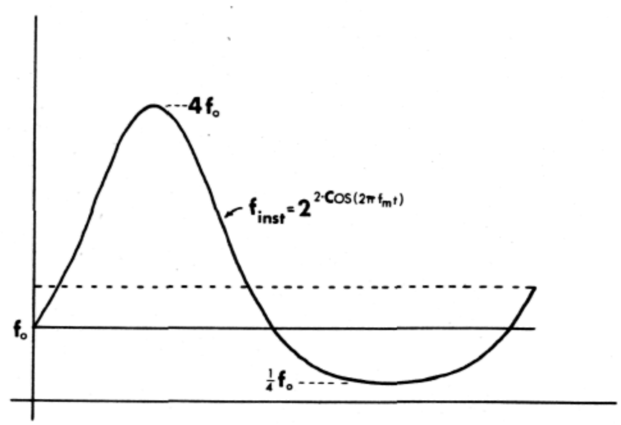

Fig. 12. Instantaneous frequency for one cycle of modulation.

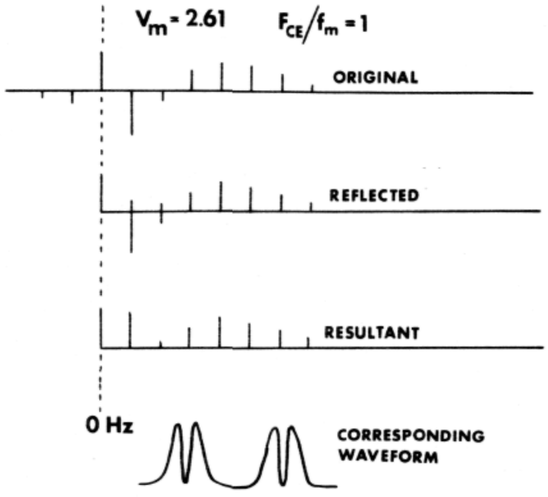

Fig. 13. Harmonic spectrum; $V_m = 2.61$, $I_0(\ln 2{\cdot}V_m) = 2$, $F_{CE} / f_m = 1$, and corresponding waveform.

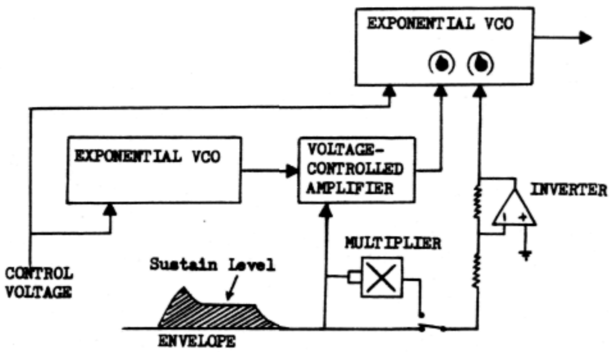

Fig. 14. Patch used to correct for pitch shift.

incomplete as the upward response to the envelope through the VCA is along the I_0 curve, while the direct path is the normal exponential. With the direct connection, complete correction is obtained only at one voltage level of the envelope, typically set at the sustain level. Incomplete correction during the attack phase often adds spectral features that enhance the musical quality of the tones. The same incomplete correction during the final decay phase, however, causes pitch variations that are generally bothersome. This can be partially remedied by using the same envelope for modulation depth control and amplitude control, and truncating the exponential tail early.

The correction can be completed to first order by squaring the envelope voltage before inverting and feeding back to the VCO. The squaring operation can usually be done with an available multiplier or "ring modulator" on the synthesizer. The normal exponential response is 2^V, so the response to V^2 goes as $1 + \ln 2{\cdot}V^2 + \cdots$ or approximately $1 + 0.69\,V^2$. The $I_0(\ln 2{\cdot}V_m)$ curve can be approximated by $1 + 0.119\,V_m{}^2 + \cdots$, so by adjusting these levels, a degree of correction can be obtained that is quite satisfactory for small modulation depths. Since a correction voltage is fed to the VCO which normally sets F_{CE} according to initial control voltages before modulation is applied, the ratio F_{CE} / f_m varies dynamically as well, and this further complicates analysis.

A second and easier to use solution is to provide a linear control input to the E-VCO to supplement normal exponential controls. Typically, an E-VCO is basically a voltage-controlled exponential current source fed to a current-controlled ramp generator (capacitor with some form of discharge, or the current can be reversed). The exponential current source uses the exponential collector current to base-emitter voltage (proportional to control voltage) response of transistors [8]. If the standing current in these exponential current sources is linearly modulated, linear FM results. This modulation is before the exponential conversion, but is a collector current modulation, not a base-emitter voltage modulation. Thus the modulation remains linear at the output; only the limits of the current excursion depend on the base-emitter voltage. If the modulating frequency is tracking the original carrier, the total excursion for fixed modulation depth of the standing current results in a constant modulation index, since both ΔF and f_m are proportional to the control voltage. This constant modulation index linear FM gives a constant sideband structure relative to the carrier and is thus a constant timbre form of linear FM, and outwardly seems the most musically useful.

Another method is to simply add a linearly modulated current to the exponential current on the way to the current-controlled oscillator. This results in a constant frequency deviation independent of control voltage, and (approximately) constant bandwidth linear FM. This same feature can also be used to offset two otherwise tracking oscillators by a fixed number of Hertz so that the beat rate between them remains independent of frequency.

Both of the above methods will result in linear FM which does not exhibit a pitch shift during dynamic depth FM. A final solution that can be added externally to existing E-VCO's is a standard logarithmic amplifier [8]. Such an amplifier must offset standard bipolar signals so that they are always positive, take Log_2 of the resulting voltage, and feed this directly to a 1 volt per octave control input. This results in constant frequency deviation linear FM, but since it is before the exponential converter, it can not be used for a linear offset. A simple log amp that can be used with existing E-VCO's is shown in Fig. 15. Fig. 16 shows how the three linear FM methods discussed above are applied to a typical E-VCO.

CONCLUSIONS

While it is possible to calculate most of the features of the FM spectrum of an E-VCO, the complexity of the calculation process and the difficulty of setting analog controls to realize a set of conditions makes everyday application of these calculations impractical. However, an understanding of the theory does provide an understanding of the sounds realized by FM techniques on standard synthesizers, and suggests that some sort of linear control should be employed when attempting to use a dynamic depth FM synthesis method. Additional thought should be given to the possibility of reversing the process so that a given spectral evolution could be realized in terms of time-dependent modulation

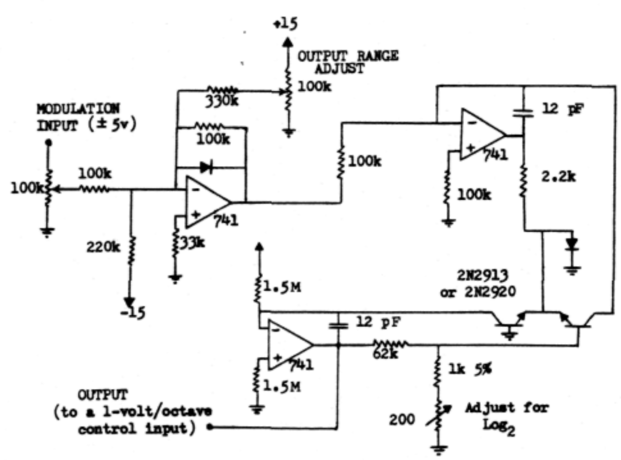

Fig. 15. Logarithmic amplifier for linear input control.

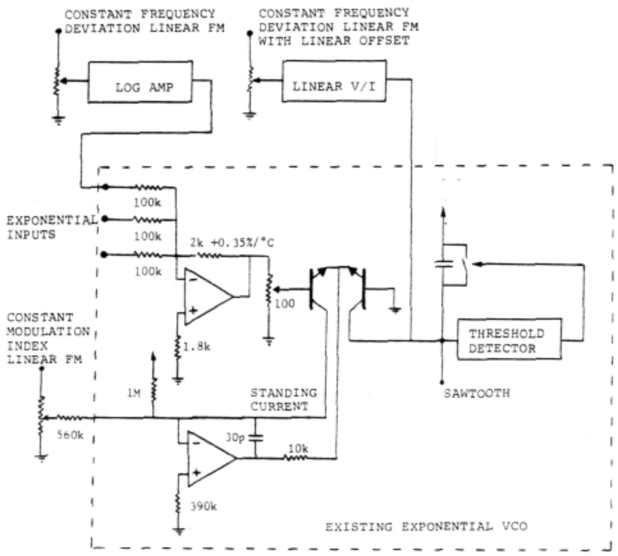

Fig. 16. Typical existing E-VCO illustrating basic methods of adding linear FM.

parameters. In this pursuit, the E-VCO with pitch pull-down correction may prove a more useful approach, as a variety of sideband distributions are possible, unlike the L-VCO which has only the one case. For general use of the dynamic depth method, simple linear controls seem the most useful.

ACKNOWLEDGMENT

The author is grateful to William Hemsath and Gordon Wilcox for valuable assistance, and for the use of equipment at the Experimental Psychology Interactive Computer Facility at Cornell University.

REFERENCES

[1] R. A. Moog, "Voltage-Controlled Electronic Music Modules," *J. Audio Eng. Soc.*, vol. 13, pp. 200-206 (July 1965).

[2] H. S. Howe, Jr., mentioned in review of Allen Strange "Electronic Music: Systems, Techniques, and Controls" in *Perspectives of New Music*, vol. 11, no. 2, p. 249 (Spring-Summer 1973).

[3] J. M. Chowning, "The Synthesis of Complex Audio Spectra by Means of Frequency Modulation," *J. Audio Eng. Soc.*, vol. 21, pp. 526-534 (Sept. 1973).

[4] M. Abramowitz and I. Stegun, *Handbook of Mathematical Functions* (Dover Publications, New York, 1965), p. 376, eq. 9.6.34.

[5] W. L. Everitt and G. E. Anners, *Communication Engineering* (McGraw-Hill, New York, 1956), p. 29.

[6] M. G. Crosby, "Carrier and Side-Frequency Relations with Multitone Frequency or Phase Modulation," *RCA Rev.* vol. 3, pp. 103-106 (July 1938).

[7] M. S. Corrington, "Variation of Bandwidth with Modulation Index in Frequency Modulation," *Proc. IRE*, vol. 35, pp. 1013-1020 (Oct. 1947).

[8] R. C. Dobkin, "Logarithmic Converters," National Semiconductor Corp., Santa Clara, Calif., Application Notes AN-30, Nov. 1969.

THE AUTHOR

Bernard A. Hutchins, Jr. was born in Rochester, NY in 1945. He received a B.S. degree in Engineering Physics from Cornell University in 1967. After three years of military service, Mr. Hutchins returned to Cornell where he is now completing graduate work. He is also the editor and publisher of *Electronotes*, a newsletter devoted to electronic music and musical engineering.

2c (19)